



Synthesis, crystal structures, and antimicrobial activities of hydrazone complexes of vanadium(V)

Shu-Jing Li, Ke Li, Xin-Jian Yao & Xiao-Yang Qiu

To cite this article: Shu-Jing Li, Ke Li, Xin-Jian Yao & Xiao-Yang Qiu (2015) Synthesis, crystal structures, and antimicrobial activities of hydrazone complexes of vanadium(V), Journal of Coordination Chemistry, 68:16, 2846-2857, DOI: [10.1080/00958972.2015.1056171](https://doi.org/10.1080/00958972.2015.1056171)

To link to this article: <http://dx.doi.org/10.1080/00958972.2015.1056171>



Accepted author version posted online: 09 Jun 2015.
Published online: 10 Jul 2015.



Submit your article to this journal [↗](#)



Article views: 70



View related articles [↗](#)



View Crossmark data [↗](#)

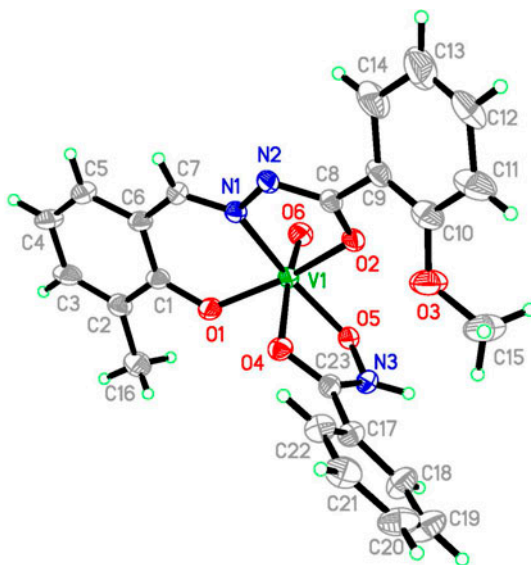
Synthesis, crystal structures, and antimicrobial activities of hydrazone complexes of vanadium(V)

SHU-JING LI[†], KE LI[†], XIN-JIAN YAO[†] and XIAO-YANG QIU^{‡*}

[†]School of Chemistry & Chemical Engineering, Zhoukou Normal University, Zhoukou, PR China

[‡]Department of Chemistry, Shangqiu Normal University, Shangqiu, PR China

(Received 4 December 2014; accepted 6 May 2015)



Two hydrazone ligands, (*E*)-*N'*-(3-bromo-2-hydroxybenzylidene)-2-methoxybenzohydrazide (HL^a) and (*E*)-*N'*-(2-hydroxy-3-methylbenzylidene)-2-methoxybenzohydrazide (HL^b), were prepared and characterized by IR, UV–vis, and ¹H NMR spectroscopy. The corresponding vanadium(V) complexes, 2[VOL^aL]·CH₃OH (1) and [VOL^bL] (2), where L is the monoanionic form of benzohydroxamic acid (HL), were prepared and characterized by IR and UV–vis spectroscopy, and single-crystal X-ray diffraction. Complex 1 crystallizes as the monoclinic space group *P*2₁/*c*, with unit cell dimensions *a* = 14.4161(16) Å, *b* = 14.0745(16) Å, *c* = 24.069(2) Å, β = 96.247(2)°, *V* = 4854.5(9) Å³, *Z* = 4, *R*₁ = 0.0541, *wR*₂ = 0.1423, *Goof* = 1.032. Complex 2 crystallizes in the orthorhombic space group *Pbca*, with unit cell dimensions *a* = 13.5906(6) Å, *b* = 18.1865(11) Å, *c* = 18.4068(11) Å, *V* = 4549.5(4) Å³, *Z* = 8, *R*₁ = 0.0549, *wR*₂ = 0.1397, *Goof* = 1.054. X-ray analysis indicates that the complexes are mononuclear octahedral vanadium(V) complexes. The thermal behavior of the complexes was investigated. The hydrazone ligands and their complexes were also evaluated for their antibacterial (*Bacillus subtilis*, *Staphylococcus aureus*, *Escherichia coli*, and *Pseudomonas fluorescens*) and antifungal (*Candida albicans* and *Aspergillus niger*) activities using the MTT (3-(4,5-

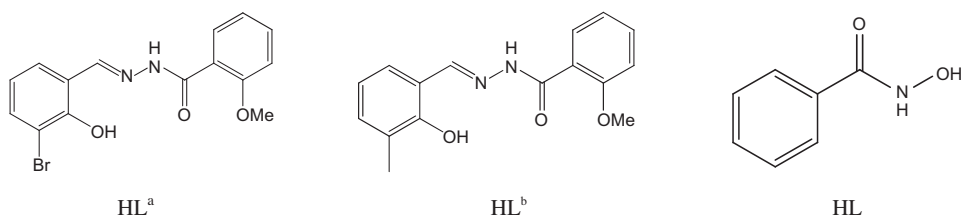
*Corresponding author. Email: xiaoyang_qiu@126.com

dimethylthiazol-2-yl)-2,5-diphenyl tetrazolium bromide) assay. The two complexes have moderate to good activities against *B. subtilis* and *S. aureus*, and **1** has moderate activity against *E. coli*.

Keywords: Hydrazone; Vanadium complex; Mononuclear complex; Crystal structure; Antimicrobial activity

1. Introduction

Hydrazones are a class of biologically active compounds prepared by condensation of carbonyl-containing compounds with hydrazides. These compounds have attracted considerable attention for their antibacterial [1–3], antifungal [4, 5], and antitumor [6, 7] activities. Hydrazone compounds bearing electron-withdrawing groups result in an improvement in their antimicrobial activities [8, 9]. Rai and coworkers reported that a series of fluoro-, chloro-, bromo-, and iodo-substituted compounds have significant antimicrobial activities [10]. Vanadium complexes with Schiff bases and hydrazones have also been reported to have interesting antibacterial activities [11–14]. As continuation of work on the exploration of complex-based antimicrobial agents, in this article, two hydrazones, (*E*)-*N'*-(3-bromo-2-hydroxybenzylidene)-2-methoxybenzohydrazide (HL^{a}) and (*E*)-*N'*-(2-hydroxy-3-methylbenzylidene)-2-methoxybenzohydrazide (HL^{b}), were prepared. The corresponding vanadium(V) complexes were also synthesized and structurally characterized, $2[\text{VOL}^{\text{aL}}]\cdot\text{CH}_3\text{OH}$ (**1**) and $[\text{VOL}^{\text{bL}}]$ (**2**), where L is the monoanionic form of benzohydroxamic acid (HL); their antimicrobial activities were investigated.



2. Experimental

2.1. Materials and methods

Vanadyl acetylacetonate and the other organic reagents were purchased from Sigma-Aldrich and used as received. All other reagents were of analytical reagent grade. Elemental analyses of C, H, and N were carried out in a Perkin–Elmer automated model 2400 Series II CHNS/O analyzer. FT-IR spectra were obtained on a Perkin–Elmer 377 FT-IR spectrometer with samples prepared as KBr pellets. UV–vis spectra were obtained on a Lambda 900 spectrometer. Thermogravimetric analyses were performed by means of a Perkin–Elmer Pyris Diamond TG-DTA from 25 and 800 °C. X-ray diffraction was carried out on a Bruker APEX II CCD diffractometer.

2.2. Synthesis of the hydrazones

The hydrazones were synthesized as follows. To a stirred methanolic solution (30 mL) of 2-methoxybenzohydrazide (0.02 mol) was added a methanolic solution (20 mL) of 3-bromosalicylaldehyde or 3-methylsalicylaldehyde (0.02 mol). The mixtures were stirred

for 30 min at room temperature and left to slowly evaporate to give colorless crystalline products, which were recrystallized from methanol and dried under vacuum in the presence of anhydrous CaCl_2 .

For HL^a: Yield 83%. IR data (cm^{-1}): 3447, 3311, 1659, 1605, 1516, 1473, 1393, 1344, 1283, 1235, 1174, 1135, 1011, 939, 793, 750, 667, 552, 518. UV–vis data (MeOH, λ_{max} , nm): 292, 328. Anal. Calcd for $\text{C}_{15}\text{H}_{13}\text{BrN}_2\text{O}_3$: C, 51.6; H, 3.7; N, 8.0. Found: C, 51.7; H, 3.9; N, 7.9%. ^1H NMR (300 MHz, d^6 -DMSO): δ 12.58 (s, 1H), 11.91 (s, 1H), 8.54 (s, 1H), 7.69 (dd, $J = 7.6, 1.7$ Hz, 1H), 7.63 (dd, $J = 7.9, 1.3$ Hz, 1H), 7.55 (m, 1H), 7.47 (dd, $J = 7.7, 1.4$ Hz, 1H), 7.20 (d, 1H), 7.09 (t, 1H), 6.91 (t, 1H), 3.90 (s, 3H). For HL^b: Yield 87%. IR data (cm^{-1}): 3453, 3305, 1651, 1608, 1525, 1470, 1398, 1353, 1292, 1245, 1172, 1152, 1020, 973, 888, 745, 521. UV–vis data (MeOH, λ_{max} , nm): 292, 332. Anal. Calcd for $\text{C}_{16}\text{H}_{16}\text{N}_2\text{O}_3$: C, 67.6; H, 5.7; N, 9.8. Found: C, 67.4; H, 5.6; N, 10.0%. ^1H NMR (300 MHz, d^6 -DMSO): δ 11.90 (s, 1H), 11.75 (s, 1H), 8.51 (s, 1H), 7.68 (dd, $J = 7.6, 1.7$ Hz, 1H), 7.54 (m, 1H), 7.3–7.0 (m, 4H), 6.85 (t, 1H), 3.90 (s, 3H), 2.04 (s, 3H).

2.3. Synthesis of the complexes

The hydrazone compounds (0.1 mmol each) and vanadyl acetylacetonate (0.1 mmol) were mixed in methanol (10 mL). The mixture was boiled under reflux for 1 h and then cooled to room temperature. Single crystals of the complexes, suitable for X-ray diffraction, were grown from the solution upon slow evaporation within a few days. The crystals were isolated by filtration, washed with methanol, and dried in vacuum containing anhydrous CaCl_2 .

Table 1. Crystallographic and refinement data for **1** and **2**.

Complex	1	2
Formula	$\text{C}_{45}\text{H}_{38}\text{Br}_2\text{N}_6\text{O}_{13}\text{V}_2$	$\text{C}_{23}\text{H}_{20}\text{N}_3\text{O}_6\text{V}$
Formula weight	1132.51	485.36
Crystal shape/color	Block/brown	Block/brown
T (K)	298(2)	298(2)
Crystal dimensions (mm^3)	$0.20 \times 0.18 \times 0.17$	$0.30 \times 0.27 \times 0.22$
Crystal system	Monoclinic	Orthorhombic
Space group	$P2_1/c$	$Pbca$
a (Å)	14.4161(16)	13.5906(6)
b (Å)	14.0745(16)	18.1865(11)
c (Å)	24.069(2)	18.4068(11)
β (°)	96.247(2)	
V (Å ³)	4854.5(9)	4549.5(4)
Z	4	8
D_{calc} (g cm^{-3})	1.550	1.417
μ (Mo $K\alpha$) (mm^{-1})	2.100	0.480
$F(0\ 0\ 0)$	2280	2000
Measured reflections	48,421	14,676
Unique reflections	9023	4233
Observed reflections [$I \geq 2\sigma(I)$]	6815	3076
Minimum and maximum transmission	0.6788 and 0.7167	0.8693 and 0.9017
Parameters	622	303
Restraints	44	1
Goodness of fit on F^2	1.032	1.054
R_1, wR_2 [$I \geq 2\sigma(I)$] ^a	0.0541, 0.1423	0.0549, 0.1397
R_1, wR_2 (all data) ^a	0.0756, 0.1608	0.0796, 0.1598

$$^a R_1 = F_o - F_c / F_o, wR_2 = \left[\sum w(F_o^2 - F_c^2) / \sum w(F_o^2) \right]^{1/2}$$

For **1**: Yield 51%. IR data (cm^{-1}): 3201 (m), 1606 (s), 1559 (w), 1525 (m), 1485 (w), 1450 (m), 1395 (w), 1341 (s), 1287 (w), 1252 (m), 1100 (w), 968 (s), 913 (w), 742 (w), 696 (w), 595 (m). UV-vis data (CH_3CN , λ_{max} , nm): 273, 337, 445. Anal. Calcd for $\text{C}_{45}\text{H}_{38}\text{Br}_2\text{N}_6\text{O}_{13}\text{V}_2$: C, 47.7; H, 3.4; N, 7.4. Found: C, 47.9; H, 3.4; N, 7.3%. For **2**: Yield 45%. IR data (cm^{-1}): 3434 (w), 3213 (w), 1602 (s), 1559 (s), 1510 (s), 1482 (m), 1433 (w), 1393 (w), 1358 (m), 1338 (m), 1272 (s), 1247 (s), 1152 (w), 1023 (w), 977 (s), 928 (w), 911 (w), 871 (m), 751 (s), 702 (s), 604 (s), 576 (m), 461 (w). UV-vis data (CH_3CN , λ_{max} , nm): 269, 333, 434. Anal. Calcd for $\text{C}_{23}\text{H}_{20}\text{N}_3\text{O}_6\text{V}$: C, 56.9; H, 4.2; N, 8.7. Found: C, 56.8; H, 4.1; N, 8.5%.

2.4. X-ray crystallography

X-ray diffraction was carried out with a Bruker APEX II CCD area diffractometer equipped with $\text{MoK}\alpha$ radiation ($\lambda = 0.71073 \text{ \AA}$). The collected data were reduced with SAINT [15]

Table 2. Selected bond distances (\AA) for **1** and **2**.

1			
V1–O1	1.860(3)	V1–O2	1.945(3)
V1–O4	1.850(3)	V1–O5	2.192(3)
V1–O6	1.584(3)	V1–N1	2.079(3)
V2–O7	1.866(3)	V2–O8	1.957(3)
V2–O10	1.852(3)	V2–O11	2.179(3)
V2–O12	1.581(3)	V2–N4	2.072(3)
C8–N2	1.295(6)	C8–O2	1.297(5)
C30–N5	1.292(6)	C30–O8	1.290(5)
O6–V1–O4	97.64(15)	O6–V1–O1	98.44(16)
O4–V1–O1	107.58(13)	O6–V1–O2	97.86(15)
O4–V1–O2	87.47(12)	O1–V1–O2	156.04(14)
O6–V1–N1	102.06(15)	O4–V1–N1	155.05(13)
O1–V1–N1	84.62(13)	O2–V1–N1	74.86(13)
O6–V1–O5	173.51(15)	O4–V1–O5	76.06(12)
O1–V1–O5	85.09(13)	O2–V1–O5	80.51(12)
N1–V1–O5	83.64(12)	O12–V2–O10	96.38(16)
O12–V2–O7	100.34(17)	O10–V2–O7	104.44(14)
O12–V2–O8	98.33(16)	O10–V2–O8	91.17(14)
O7–V2–O8	154.04(14)	O12–V2–N4	99.51(16)
O10–V2–N4	160.27(14)	O7–V2–N4	84.18(14)
O8–V2–N4	75.05(13)	O12–V2–O11	172.84(16)
O10–V2–O11	76.69(13)	O7–V2–O11	83.34(14)
O8–V2–O11	80.21(13)	N4–V2–O11	86.93(13)
2			
V1–O1	1.849(2)	V1–O2	1.981(2)
V1–O4	2.211(2)	V1–O5	1.854(2)
V1–O6	1.589(3)	V1–N1	2.065(3)
C8–N2	1.308(4)	C8–O2	1.285(4)
O6–V1–O1	99.86(13)	O6–V1–O5	96.93(12)
O1–V1–O5	108.42(11)	O6–V1–O2	100.27(12)
O1–V1–O2	152.79(11)	O5–V1–O2	87.07(10)
O6–V1–N1	98.66(12)	O1–V1–N1	84.12(11)
O5–V1–N1	157.97(11)	O2–V1–N1	74.91(10)
O6–V1–O4	173.30(11)	O1–V1–O4	83.07(11)
O5–V1–O4	76.40(9)	O2–V1–O4	78.98(9)
N1–V1–O4	87.61(10)		

and a multi-scan absorption correction was performed using SADABS [16]. The structures of the complexes were solved by direct methods and refined against F^2 by full-matrix least-squares using SHELXTL [17]. All non-hydrogen atoms were refined anisotropically. The amino hydrogens were located from electron density maps and refined isotropically. The remaining hydrogens were placed in calculated positions and constrained to ride on their parent atoms. There are 44 restraints in the refinement of **1**, which arises from the isotropic treatment of carbons C37, C39, C40, C41, C42, C43, and C45 with relative high thermal ellipsoids, and from the restriction (0.90(1) Å) of the amino N–H bond lengths. The crystallographic data and refinement parameters for the compounds are listed in table 1. Selected bond lengths and angles are listed in table 2.

2.5. Antimicrobial assay

The antibacterial activities of the hydrazone ligands and the vanadium complexes were tested against *Bacillus subtilis*, *Staphylococcus aureus*, *Escherichia coli*, and *Pseudomonas fluorescens* using MH (Mueller–Hinton) medium. The antifungal activities of the compounds were tested against *Candida albicans* and *Aspergillus niger* using RPMI-1640 medium. The MIC values of the tested compounds were determined by a colorimetric method using the dye MTT [18]. A stock solution of the compound (150 µg mL⁻¹) in DMSO was prepared and varying amounts (75, 37.5, 18.8, 9.4, 4.7, 2.3, 1.2, and 0.59 µg mL⁻¹) were added to the appropriate sterilized liquid medium. A specified quantity of the medium containing the compound was poured into micro-titration plates. A suspension of the microorganism was prepared to contain approximately 1.0×10^5 cfu mL⁻¹ and applied to micro-titration plates with serially diluted compounds in DMSO to be tested and incubated at 37 °C for 24 h and 48 h for bacterial and fungi, respectively. The MIC values were visually determined on each of the micro-titration plates and 50 µL of PBS (phosphate-buffered saline 0.01 mol L⁻¹, pH = 7.4) containing 2 mg mL⁻¹ MTT was added to each well. Incubation was continued at room temperature for 4–5 h. The content of each well was removed, and 100 µL isopropanol containing 5% 1 mol L⁻¹ HCl was added to extract the dye. After 12 h of incubation at room temperature, the optical density was measured with a microplate reader at 550 nm.

3. Results and discussion

3.1. Synthesis and characterization

HL^a and HL^b were readily prepared by condensation of a 1:1 M ratio of 2-methoxybenzohydrazide with 3-bromosalicylaldehyde and 3-methylsalicylaldehyde, respectively, in methanol. Complexes **1** and **2** were prepared by reaction of the hydrazone ligands with vanadyl acetylacetonate in methanol, followed by recrystallization. Elemental analysis results of the complexes are in accord with the molecular structures proposed by X-ray crystallography.

3.2. Spectroscopic studies

In IR spectra of the hydrazone ligands and the complexes, the weak and broad bands centered at ~ 3440 cm⁻¹ are assigned to O–H stretches. The weak and sharp bands located at ~ 3310 cm⁻¹ for the hydrazone ligands and 3210 cm⁻¹ for the complexes are assigned to

N–H stretches. The position of the bands demonstrates that the N–H hydrazone protons are engaged in hydrogen bonding. The intense bands at 1659 cm^{-1} for HL^a and 1651 cm^{-1} for HL^b arise from $\nu(\text{C}=\text{O})$ vibrations, whereas the bands at $\sim 1606\text{ cm}^{-1}$ can be assigned to $\nu(\text{C}=\text{N})$. The absence of $\nu(\text{C}=\text{O})$ bands for the complexes indicates enolization of the amide functionality occurs upon coordination of the ligands to the V(V) center. Strong bands at 1603 cm^{-1} for **1** and 1602 cm^{-1} for **2** are observed, which can be attributed to the asymmetric stretching vibration of the conjugated $\text{CH}=\text{N}=\text{N}=\text{C}=\text{O}$ groups, characteristic for coordination of the enolate form of the ligands. The strong $\nu(\text{V}=\text{O})$ bands at 968 cm^{-1} for **1** and 977 cm^{-1} for **2** could be clearly observed for both complexes [19].

In electronic spectra of the complexes, the lowest energy transitions at 445 nm for **1** and 434 nm for **2** can be attributed to LMCT transitions, since charge transfer occurs from the oxygen's p-orbital occupied by the lone pair of the ligand to the empty d-orbital of

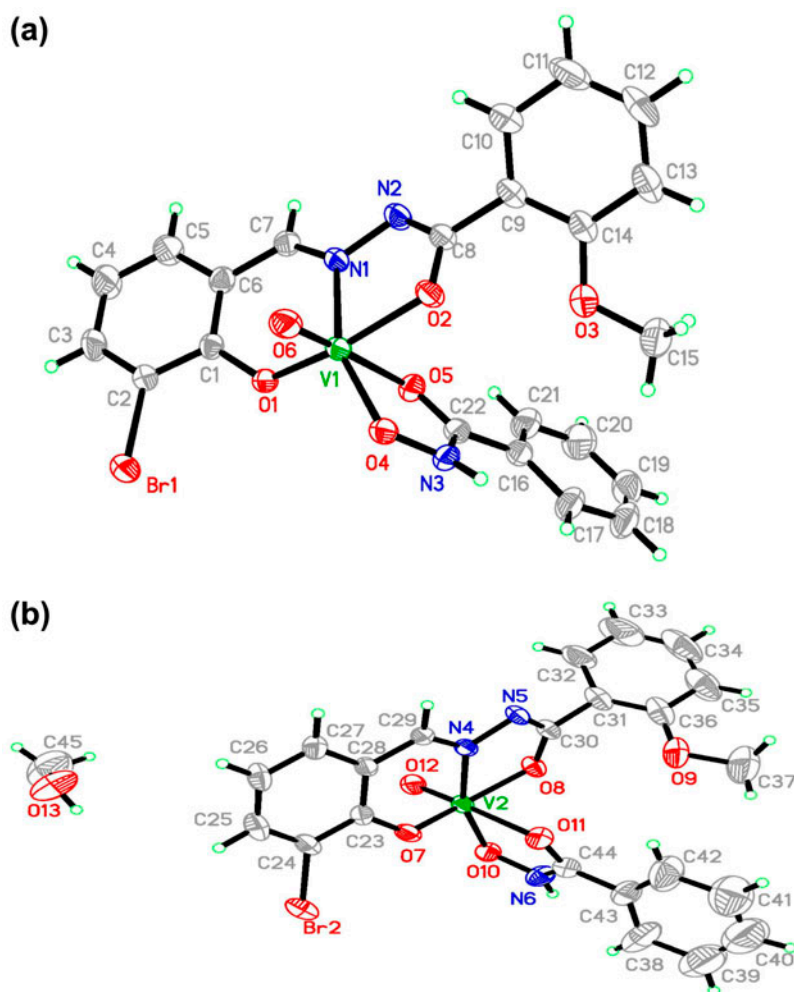


Figure 1. (a) A perspective view of V1 of **1** with the atom-labeling scheme. Thermal ellipsoids are drawn at the 30% probability level and (b) A perspective view of V2 and the methanol of **1** with the atom-labeling scheme. Thermal ellipsoids are drawn at the 30% probability level.

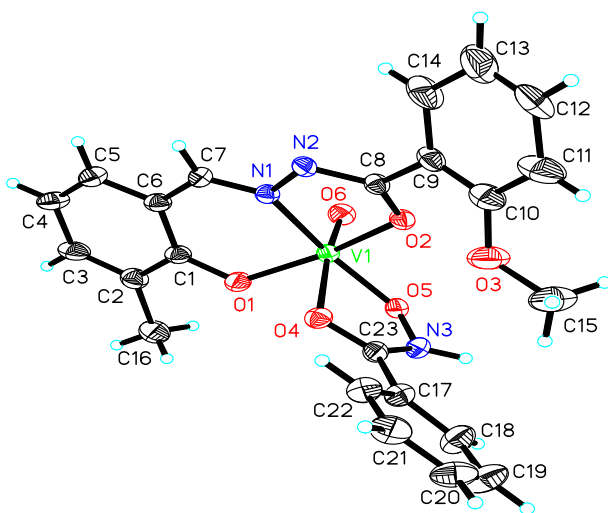


Figure 2. A perspective view of **2** with the atom-labeling scheme. Thermal ellipsoids are drawn at the 30% probability level.

vanadium. The other strong bands in the 320–340 nm range for both complexes are similar to the absorption bands in spectra of the corresponding hydrazone ligands, so they are attributed to intra-ligand $\pi \rightarrow \pi^*$ transitions of the ligands. The other mainly LMCT and to some extent $\pi \rightarrow \pi^*$ bands are at 273 nm for **1** and 269 nm for **2**, due to the oxygen donors bound to vanadium(V) [19].

3.3. Structure description of the complexes

The molecular structures of **1** and **2** are shown in figures 1 and 2, respectively. The asymmetric unit of **1** contains two vanadium complexes and one methanol of crystallization. The coordination geometry around vanadium is distorted octahedral with the tridentate hydrazone coordinated meridional, forming five- and six-membered chelate rings with bite angles of $74.86(13)^\circ$ (**1**) and $74.91(10)^\circ$ (**2**) (N1–V1–O2), and $84.62(13)^\circ$ (**1**) and $84.12(11)^\circ$ (**2**) (N1–V1–O1), respectively, typical for this type of ligand system [20]. Each chelating hydrazone ligand lies in a plane with one hydroxylato ligand which lies *trans* to the hydrazone imino N. One carbonyl of the benzohydroxamate ligand *trans* to the oxo group completes the distorted octahedral coordination sphere at a rather elongated distance of 2.2 Å, due to the *trans* influence of the oxo group. This is accompanied by a significant displacement of vanadium from the plane defined by the four basal donors toward the apical oxo oxygen by 0.29(1) Å. The hydrazones coordinate in their doubly deprotonated enolate form, consistent with the observed O2–C8 and N2–C8 bond lengths of 1.297(5) and 1.295(6) Å in **1**, and 1.285(4) and 1.308(4) Å in **2**, respectively. This agrees with reported bond lengths for vanadium with the enolate form of this ligand type [20–22]. In the crystal packing structure of **1**, hydrazone molecules are linked by methanol molecules through intermolecular hydrogen bonds of N–H \cdots O, O–H \cdots N, and N–H \cdots N, leading to the formation of 2-D layers parallel to the *bc* direction (figure 3). In the crystal packing structure of **2**, hydrazone molecules are linked through intermolecular hydrogen bonds of N–H \cdots N, leading to the formation of 1-D chains along the *a* axis (figure 4).

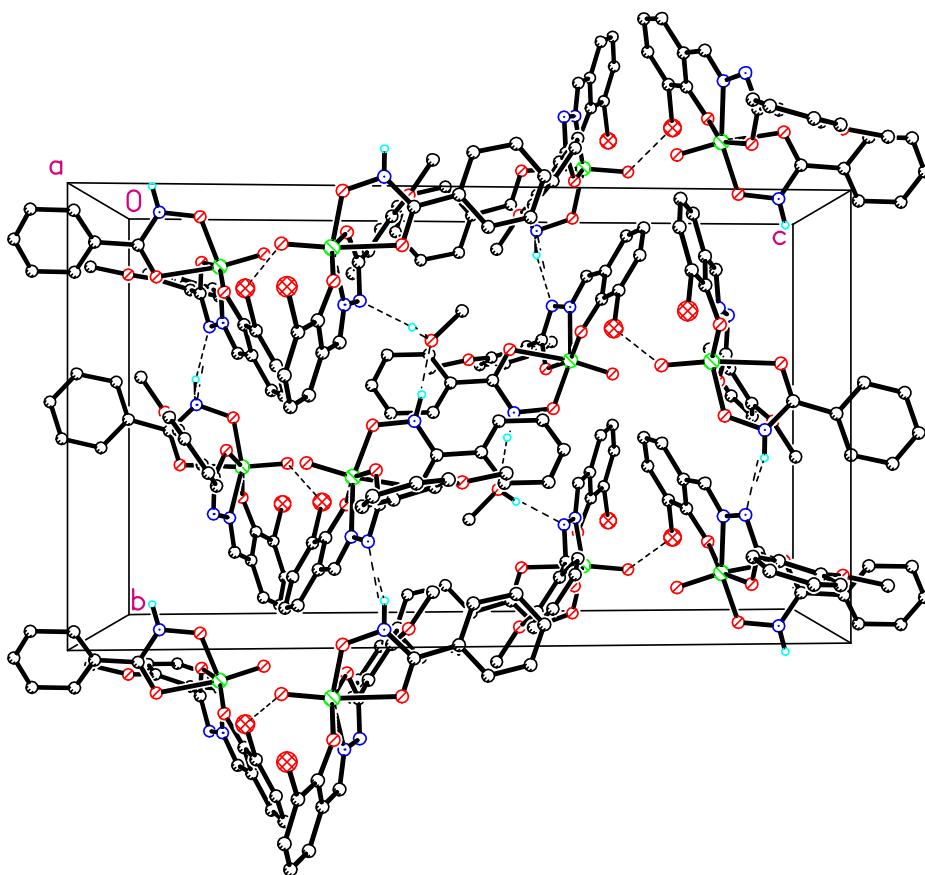


Figure 3. Molecular packing structure of **1** with hydrogen bonds shown as dotted lines.

3.4. Thermogravimetric analyses of the complexes

TG curves of **1** and **2** are shown in figures 5 and 6, respectively. Complex **1** decomposes in two steps, one step from 183 to 233 °C and the second step from 233 to 423 °C. The first step represents the loss of the benzohydroxamate ligand, with a mass loss of 24.3%, in accord with the calculated value of 24.7%. The second step represents the loss of the hydrazone ligand and formation of V_2O_5 . The total mass loss of 83.3% agrees well with the calculated value of 83.5%. Complex **2** decomposes in two steps, one step from 168 to 260 °C and the second step from 260 to 514 °C. The first step represents the loss of the benzohydroxamate ligand, with a mass loss of 28.3%, in accord with the calculated value of 28.0%. The second step represents the loss of the hydrazone ligand and formation of V_2O_5 . The total mass loss of 82.5% agrees well with the calculated value of 81.9%.

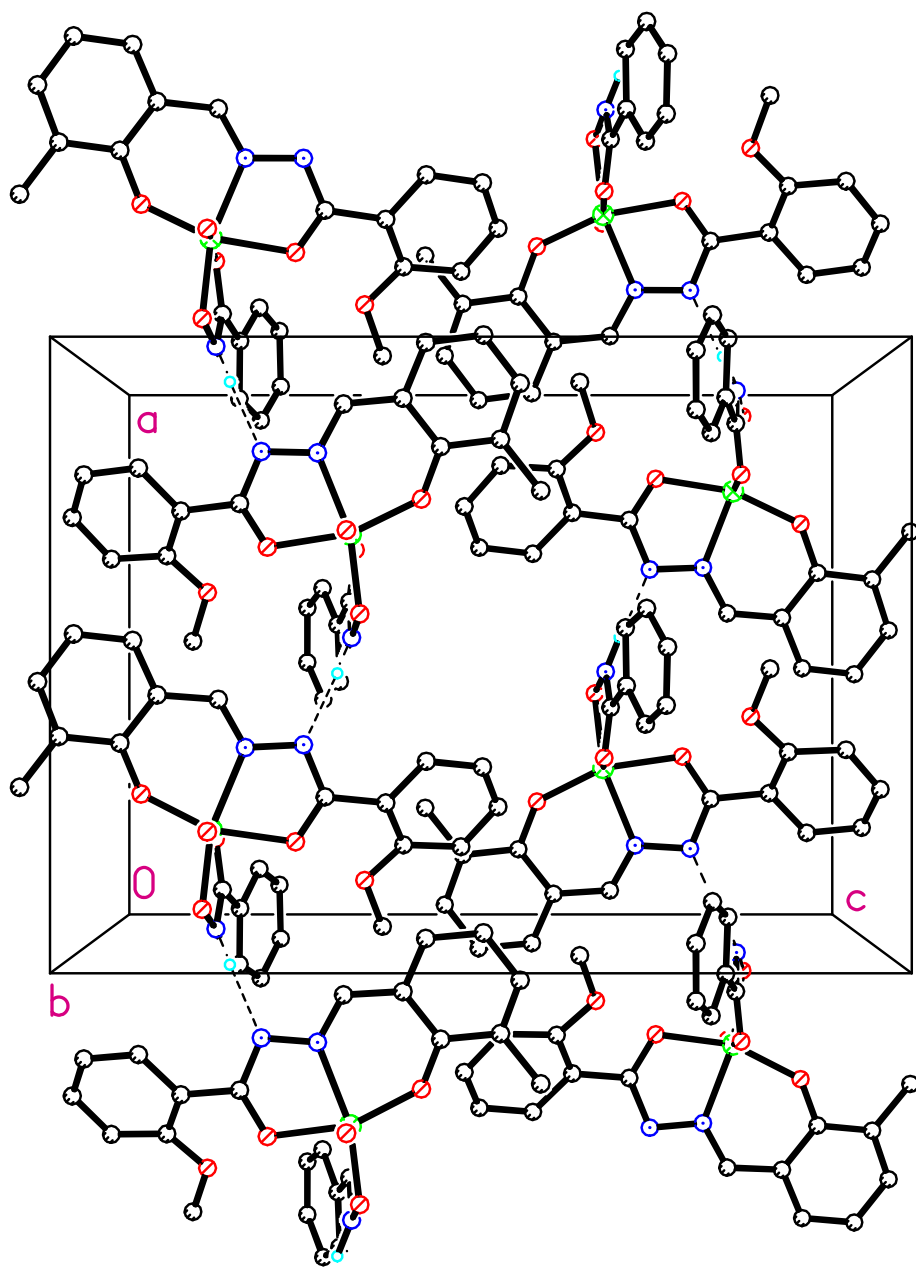


Figure 4. Molecular packing structure of **2** with hydrogen bonds shown as dotted lines.

3.5. Antimicrobial activity

The hydrazone ligands and their vanadium complexes were screened for antibacterial activities against two Gram (+) bacterial strains (*B. subtilis* and *S. aureus*) and two Gram (-) bacterial strains (*E. coli* and *P. fluorescence*) using the MTT method. The MIC (minimum

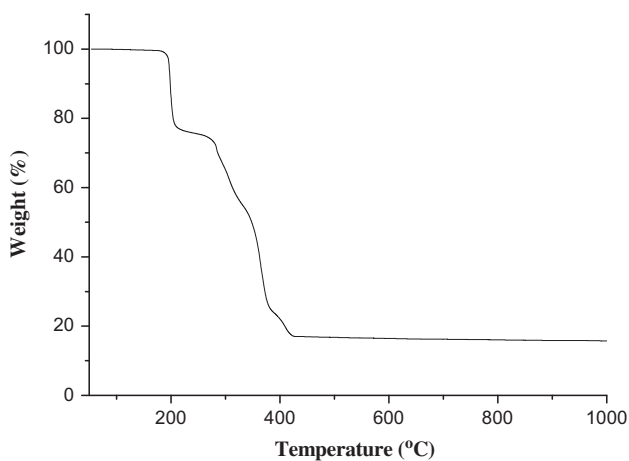
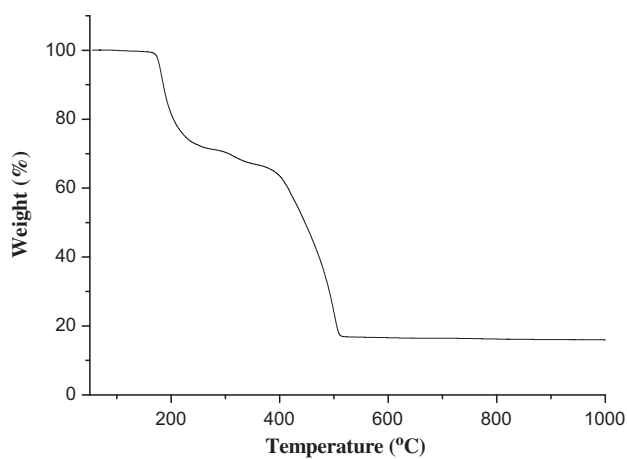
Figure 5. TG curve of **1**.Figure 6. TG curve of **2**.

Table 3. Antimicrobial activities of the hydrazone ligands and their vanadium complexes.

Compound	Minimum inhibitory concentrations ($\mu\text{g mL}^{-1}$)		
	<i>B. subtilis</i>	<i>S. aureus</i>	<i>E. coli</i>
HL ^a	9.4	9.4	18.8
HL ^b	9.4	18.8	37.5
1	4.7	9.4	75
2	9.4	37.5	>150
Penicillin G	2.3	4.7	>150

inhibitory concentration, $\mu\text{g mL}^{-1}$) values of the compounds against four bacteria are listed in table 3. Penicillin G was used as the standard drug control. The hydrazone compounds show moderate activities against the bacteria *B. subtilis*, *S. aureus*, and *E. coli* and no activity against *P. fluorescens*. The two complexes have moderate to good activities against *B. subtilis* and *S. aureus*. Complex **1** has moderate activity against *E. coli*, while **2** has no activity. Both complexes have no activity against *P. fluorescens*. In general, **1** has stronger activities against *B. subtilis*, *S. aureus*, and *E. coli* than **2**. The ligands and complexes show no activity against *P. fluorescens* and two fungal strains (*C. albicans* and *A. niger*).

Supplementary material

CCDC – 1036936 for **1** and 1036937 for **2** contain the supplementary crystallographic data for this paper. These data can be obtained free of charge at <http://www.ccdc.cam.ac.uk/const/retrieving.html> or from the Cambridge Crystallographic Data Centre (CCDC), 12 Union Road, Cambridge CB2 1EZ, UK; Fax: +44(0)1223-336033 or Email: deposit@ccdc.cam.ac.uk.

Disclosure statement

No potential conflict of interest was reported by the authors.

Funding

This work was supported by the Educational Commission of Henan Province of China [grant number 14B150036]; Natural Science Foundation of Henan Province of China [grant number 142300410252].

References

- [1] Z.A. Kaplancikli, M.D. Altintop, A. Ozdemir, G. Turan-Zitouni, G. Goger, F. Demirci. *Lett. Drug Des. Discov.*, **11**, 355 (2014).
- [2] R. Narisetty, K.B. Chandrasekhar, S. Mohanty, B. Balram. *Lett. Drug Des. Discov.*, **10**, 620 (2013).
- [3] F. Zhi, N. Shao, Q. Wang, Y. Zhang, R. Wang, Y. Yang. *J. Struct. Chem.*, **54**, 148 (2013).
- [4] A. Özdemir, G. Turan-zitouni, Z.A. Kaplancikli, F. Demirci, G. Iscan. *J. Enzyme Inhib. Med. Chem.*, **23**, 470 (2008).
- [5] C. Loncle, J.M. Brunel, N. Vidal, M. Dherbomez, Y. Letourneux. *Eur. J. Med. Chem.*, **39**, 1067 (2004).
- [6] Y.-C. Liu, H.-L. Wang, S.-F. Tang, Z.-F. Chen, H. Liang. *Anticancer Res.*, **34**, 6034 (2014).
- [7] P. Krishnamoorthy, P. Sathyadevi, A.H. Cowley, R.R. Butorac, N. Dharmaraj. *Eur. J. Med. Chem.*, **46**, 3376 (2011).
- [8] M. Zhang, D.-M. Xian, H.-H. Li, J.-C. Zhang, Z.-L. You. *Aust. J. Chem.*, **65**, 343 (2012).
- [9] L. Shi, H.-M. Ge, S.-H. Tan, H.-Q. Li, Y.-C. Song, H.-L. Zhu, R.-X. Tan. *Eur. J. Med. Chem.*, **42**, 558 (2007).
- [10] N.P. Rai, V.K. Narayanaswamy, T. Govender, B.K. Manuprasad, S. Shashikanth, P.N. Arunachalam. *Eur. J. Med. Chem.*, **45**, 2677 (2010).
- [11] S.S. Wazalwar, N.S. Bhave, A.G. Dikundwar, P. Ali. *Synth. React. Inorg. Met.-Org. Nano-Met. Chem.*, **41**, 459 (2011).
- [12] J.-L. Liu, M.-H. Sun, J.-J. Ma. *Synth. React. Inorg. Met.-Org. Nano-Met. Chem.*, **45**, 117 (2015).
- [13] Z.H. Chohan, S.H. Sumrra, M.H. Youssoufi, T.B. Hadda. *Eur. J. Med. Chem.*, **45**, 2739 (2010).
- [14] O. Taheri, M. Behzad, A. Ghaffari, M. Kubicki, G. Dutkiewicz, A. Bezaatpour, H. Nazari, A. Khaleghian, A. Mohammadi, M. Salehi. *Transit. Met. Chem.*, **39**, 253 (2014).

- [15] Bruker. *SMART (Version 5.625) and SAINT (Version 6.01)*, Bruker AXS Inc., Madison, Wisconsin, USA (2007).
- [16] G.M. Sheldrick. *SADABS, Program for Empirical Absorption Correction of Area Detector*, University of Göttingen, Germany (1996).
- [17] G.M. Sheldrick, *SHELXTL V5.1 Software Reference Manual*, Bruker AXS Inc., Madison, Wisconsin, USA (1997).
- [18] J. Meletiadis, J.F.G.M. Meis, J.W. Mouton, J.P. Donnelly, P.E. Verweij. *J. Clin. Microbiol.*, **38**, 2949 (2000).
- [19] A. Sarkar, S. Pal. *Polyhedron*, **26**, 1205 (2007).
- [20] H.H. Monfared, S. Alavi, R. Bikas, M. Vahedpour, P. Mayer. *Polyhedron*, **29**, 3355 (2010).
- [21] X.-T. Zhang, X.-P. Zhan, D.-M. Wu, Q.-Z. Zhang, S.-M. Chen, Y.-Q. Yu, C.-Z. Lu. *Chin. J. Struct. Chem.*, **21**, 629 (2002).
- [22] H.H. Monfared, S. Alavi, R. Bikas, M. Vahedpour, P. Mayer. *Polyhedron*, **29**, 3355 (2010).